

# High optical quality models for flow visualization and PIV measurement

Milos Kasperek<sup>1\*</sup>, and Ludmila Novakova<sup>1</sup>

<sup>1</sup>J.E. Purkyně University in Usti nad Labem, Institute of Machinery and Energetics, 40096 Usti nad Labem, Czech Republic

**Abstract.** Visualization of internal flow or PIV measurements in areas of real pipe elements is a method commonly used in flow studies. For these applications, transparent models with very complex internal geometries are required. Key features of the model are the high-quality optical access, which ideally allows to obtain image of the whole measured area without deformation and with noise suppression. The technology of 3d printing in combination with casting allows the production of almost any type of transparent models of piping elements. Models produced using this technique have almost ideal optical properties. By using index-matching fluid, optical distortions as well as reflections and refractions of light on the inner edges of the model are suppressed. The paper presents the results of visualization and 2D PIV measurements in the model of the globe valve with adjustable valve plug. The valve's inner geometry was rapid prototyped using a water-soluble material and casted with clear silicone Sylgard 184 under vacuum. The model exhibits excellent optical properties for PIV measurements, especially in the vicinity of walls.

## 1 Introduction

In fluid mechanics and in applications related to the flow of any transparent fluid, the PIV (Particle Image Velocimetry) method is often used. There are several preconditions for the successful application of the PIV method for internal flow of liquids [1]. It is necessary to use seeding particles that are able to track the fluid motion faithfully over a given range of velocities and accelerations. The illumination of the measuring plane must be sufficiently intensive and uniform. Optical access to the entire measured area is very important and the measuring area has to be captured by a camera with sufficient spatial resolution and light sensitivity. In summary, ideally a completely transparent model must be made without visible joints in the laser light path or camera's vision path. In addition to these requirements, we can add at least partial heat and chemical resistance and durability of the model material.

Currently, two methods of producing transparent models with complex geometry are commonly used [2]. The first is direct 3D printing of models from transparent materials, either by stereolithography or using PolyJet methods [3]. Stereolithography can achieve better surface quality but cannot print with a different material as support. PolyJet allows printing with a support material. The most commonly used materials for transparent models are Vero Clear resin and water-soluble support material. We have used the second technique, more labour-intensive, which brings the benefit of excellent optical quality of the models, affordability and the ability to produce any

complex geometry [4,5]. The disadvantage of the presented technique is a slight inaccuracy in the final dimensions of the model due to the manual modification of the surface of the 3D print. For the purpose of visualization and measurement by PIV, a globe valve model was cast and completed with functional elements.

## 2 Manufacturing technique

### 2.1 Manufacture of the casting

The process of manufacturing of the presented transparent flow phantom of the globe valve is a combination of two technologies: casting and additive technology (3D printing). First, a mould of the valve's inner geometry is produced using 3D printing. This mould serves as the inner core during casting. Fused Filament Fabrication (FFF) 3D printing method was used with polyvinyl alcohol (PVA) as the filament. This material was chosen because of its water solubility. The printed surface of the inner core is not of sufficient quality and therefore the surface needs to be altered. Surface treatment is carried out by applying a solution of water and filament to smooth out surface irregularities. After surface preparation, the core of the valve is placed in the prepared container. This creates a mould for casting of the transparent phantom globe valve. Clear silicone resin is then poured into the mould and the mould is placed in a vacuum oven. After the clear silicone resin is solidified, the core is removed from the mould with water. The clear silicone resin used is a commercial variant of polydimethylsiloxane (PDMS)

\* Corresponding author: [milos.kasperek@ujep.cz](mailto:milos.kasperek@ujep.cz)

Sylgard 184. Sylgard 184 was used for its high-quality optical properties, in particular for its low refractive index (1.412 RI).

## 2.2 Functional components

The functional part of the globe valve model can be divided into five parts: the packing, the connecting shaft, the packing nut, the valve stem with the plug and hand wheel. The packing, the packing nut, connecting shaft and the hand wheel are made by 3D printing. The plug with the valve stem is made by a combination of 3D printing and casting technology - the stem is made by 3D printing, the plug by casting. As it subsequently turned out, the FFF 3D printing method is not suitable for the production of the functional parts of the valve, because liquid leakage between the printed layers. As a result, the functional parts were printed again, but using the stereolithography 3D printing method (SLA) to eliminate the leak problem. Thanks to the 3D printing quality of SLA, all functional parts can be printed in detail, including stem. To produce the plug with the valve stem, a PVA plug mould was printed using FFF 3D printing and its surface was modified. The printed stem was inserted into this mould. Silicone resin was poured into the mould and bubbles were removed from the resin using a vacuum oven. After the silicone resin was cured, the mould was dissolved using water. All the functional parts of the valve were assembled and inserted into the globe valve phantom. A schematic of the globe valve is shown in Figure 1.

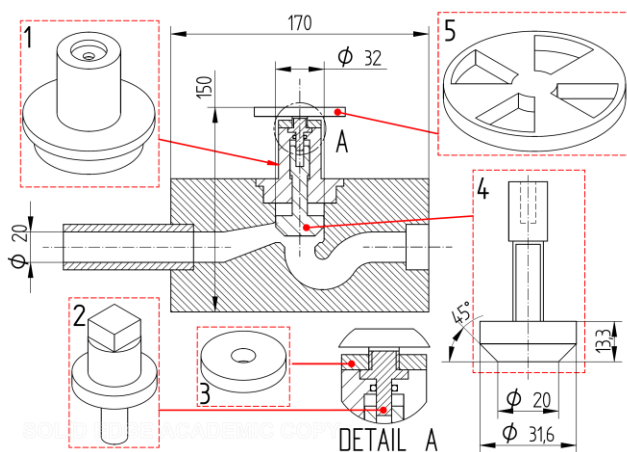


**Fig. 1.** Scheme of globe valve. The transparent body of the globe valve houses the functional parts of the model. The numbered positions represent the functional parts of the model: 1. Packing, 2. Connecting shaft, 3. Packing nut, 4. Stem with plug, 5. Hand wheel.

## 3 Experimental setup

Standard 2D PIV measurement and flow visualization were performed. The measurement plane for both PIV and visualization was placed in the axial plane of the globe valve model. For the measurement of velocity profiles by the PIV method, the fluid was seeded by glass hollow silver-coated particles of 10  $\mu\text{m}$ , and a 532 nm camera

filter was employed to minimize glare effects. For visualization, fluorescent particles (with fluorescent dye Rhodamine B:) of 50-100 micrometres were used and the signal was filtered with a 554 nm camera filter.

The aim of our measurements was to obtain the best quality data with the minimum optical distortion. For this reason, an index matching fluid was used [6,7]. It means that the liquid closely matches the refractive index of the model material. The magnitude of the optical deformation for water as a working fluid is shown in Fig. 2. The working fluid was a mixture of water and glycerine. The refractive index of Sylgard 184 is given by the manufacturer as 1.415 (Ri). This value can be influenced by curing time and temperature. The resulting optimum working fluid is mixed as a 40:60 weight ratio of water and glycerine. The resulting refractive index of the mixture is 1.4176 (Ri) [8]. The refractive index of the working fluid was examined refractometrically and visually. The refractive index measured by the refractometer was 1.412 (Ri). No optical distortion is evident from the visual inspection in Figure 3.

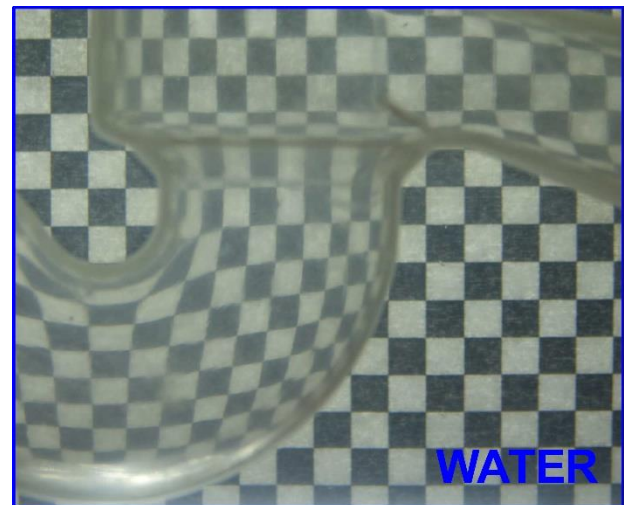


**Fig. 2.** Visual inspection of the optical deformation in the measured area using water (1.33 Ri) as the working fluid.



**Fig. 3.** Visual inspection of the optical deformation in the measured area using water-glycerine mixture (1.41 Ri) as the working fluid.

The optical properties of the model were tested by measuring of axial velocity profiles in a narrow section with laminar flow regime. The measurements were performed with both refractive matching fluid and water. This procedure allowed to quantify the effect of optical deformations when compared with the analytical result of the parabolic laminar profile. The results (Fig 4) show that the deformation of the optical profile near the wall is significantly suppressed in index matching fluid

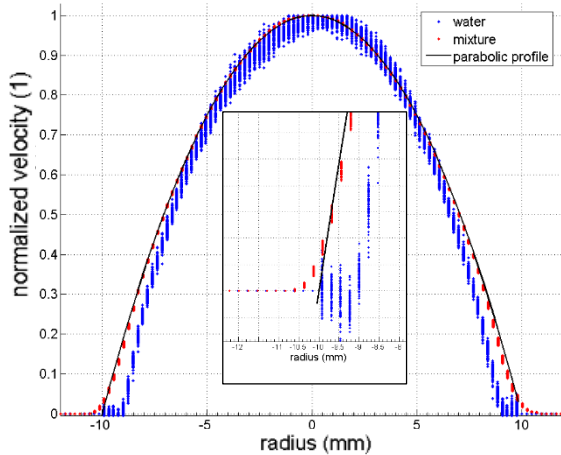


**Fig. 4.** Parabolic axial velocity profile in narrow section. The blue data represents data measured with water as working fluid, the red data with a mixture of water and glycerine. The black curve is obtained by analytical solution.

compared to water. The graph shows the result of the measurement of 30 velocity profiles along the narrow section. The velocity profiles of the index matching fluid are very close to the theoretical laminar profile. A significant deviation occurs at a distance of about 0.3 - 0.4 mm from the wall. At this distance, the deviation from the analytical solution is due to both optical deformation near the wall and particle-wall interaction. The results obtained with water show a more pronounced deviation from the theoretical profile. The typical “reduced” shape of velocity profile arises from optical deformation when the refractive index of the liquid is lower than the index of the model. The plot in Fig. 5 shows a histogram of the x-velocity uncertainties for both liquids. The histogram confirms the significantly smaller measurement uncertainties when using the water-glycerine solution as

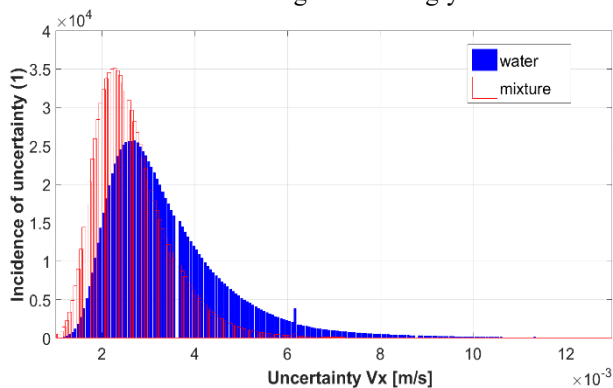


**Fig. 5.** Histogram of the x-velocity uncertainties. The blue columns represent the uncertainty distribution for water. Red columns represent the uncertainty distribution for index matching fluid.

the working fluid. The histogram for water shows the higher uncertainty values, which are probably associated with image distortion near the wall.

## 4 Results

The quality of the flow visualization in the axial plane of the globe valve model shows very good potential for flow studies. Visualization was performed again with both working fluids, water and a mixture of water and glycerine (Fig. 6 and 7).

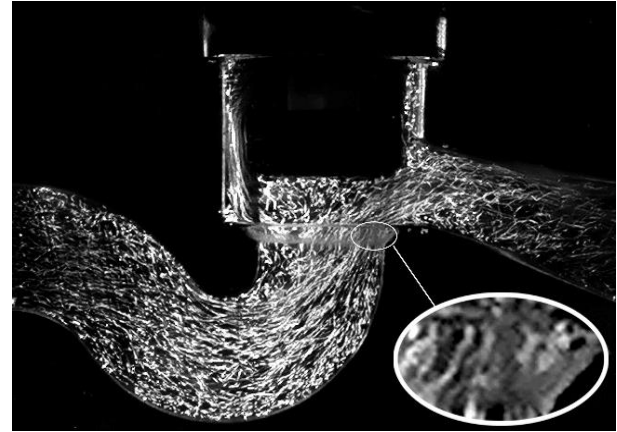


**Fig. 6.** Visualization in the axial plane of the model. Working fluid was the water (Ri 1.33).

The model showed remarkably good optical properties. The illumination of the laser sheet is homogeneous over the entire area under study. This indicates that the model material is optically homogeneous, with a minimum of bubbles, which are a common part of cast models. The detail in the images shows the reduction of particle visibility near the edge of the model. For water, this reduction in transparency is much more significant (Fig. 6). From the image of the mixture flow (Fig. 7), the flow can be very well analysed. From the flow pattern, regions of significant 3d flow as

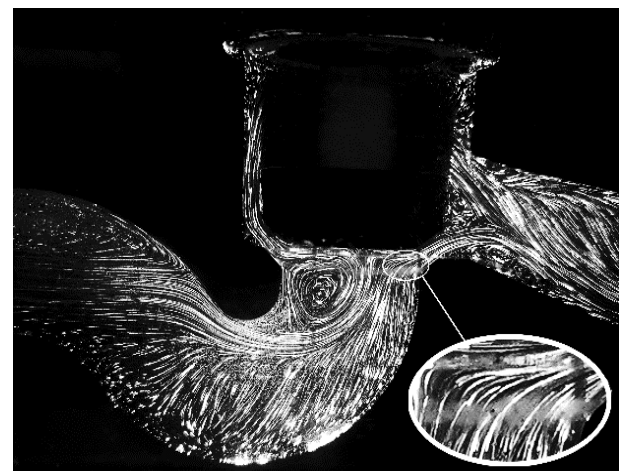


**Fig. 7.** Visualization in the axial plane of the model. Working fluid was the mixture of water and glycerine (Ri 1.41).

well as vortices under the cone and in the outlet can be clearly identified. The visualization was performed on a model with an opaque plug. For the PIV measurements, this model was upgraded and the plug replaced with a transparent and tighter one. The new plug was made of Sylgard 184. PIV measurements confirmed the suitability of the model for optical methods. With a standard 2D PIV setup, it was possible to use adaptive correlation with an interrogated area of 8x8 pixels. For example, we obtained more than 80 values in the input velocity profile. Even at locations close to the edges of the model, the data were not significantly negatively affected. Despite the use of common non-fluorescent particles, no disturbing reflections were visible near the walls. Several regimes with different plug positions were measured. Fig. 8 shows the measurement results of two regimes. In Figure 8a, the detail of the leaking plug is clearly visible.

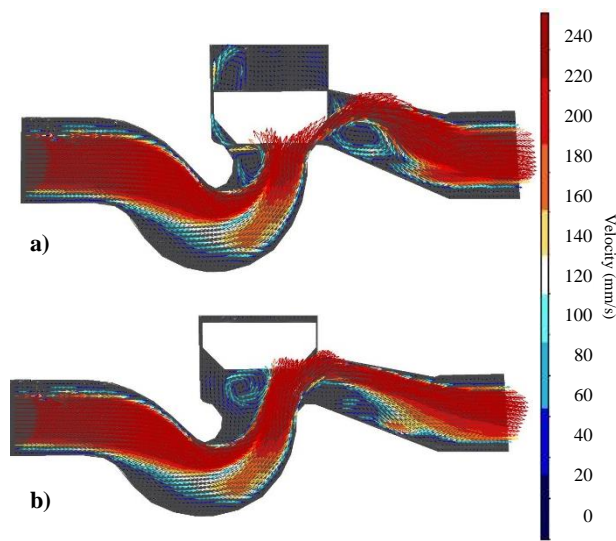


**Fig. 8.** Results of PIV measurements in the axial plane. Two regimes with the same flow rate but different plug position.

## 5 Discussion

The described method of manufacturing of transparent models ensures excellent optical access without significant optical distortion. The combination of 3d printing and casting enables to produce a cavity even with a very complex geometry. This technique is often used for medical applications, since data for 3D printing can be easily converted from medical imaging methods. As can be seen from our model, these castings can be supplemented with additional features that provide other functions of the model, such as the closing of the plug. These parts can be also made transparent to provide optical access to other parts of the model. We have verified that even in the case of a very complex geometry of the model, the optical access to the measured areas is very good. Our work has confirmed that 3D printing is an effective tool in producing models for PIV measurements, including functional parts of the models.

## Acknowledgements

This work was supported by grant within student grant competition at UJEP - Jan Evangelista Purkyně University in Ústí nad Labem, project No.: UJEP-SGS-2020-48-003-2.

This work was supported by grant within student grant competition at UJEP - Jan Evangelista Purkyně University in Ústí nad Labem, project No.: UJEP-SGS-2021-48-003-2

## References

1. Novotny, J., Machovska, I, Acta Polytech., **58**, (2018)
2. Yazdi, S., P. Geoghegan, P. Docherty, M. Jermy, A. Khanafer, Ann. Biomed. Eng. **46**(11), (2018)
3. W. H. Ho, I. J. Tshimanga, M. N. Ngoepe, M. C. Jermy & P. H. Geoghegan, Cardiovasc. Eng. Technol, **11** (2020)
4. Hopkins, L., J. Kelly, A. Wexler, and A. Prasad., Exp. Fluids, **29** (2000)
5. C. J. T. Spence, N. A. Buchmann, M. C. Jermy, S. M. Moore, Exp Fluids, **50** (2011)
6. Yousif, M.Y., Holdsworth, D.W., Poepping T.L, Exp Fluids, **50**, 2011
7. Miller P., Danielson K., Moody G., Slifka A., Drexler E., Hertyberg J., Exp Fluids, **41**, 2006.
8. Takamura K., Fisher H., Morrow N.R., J. Pet. Sci. Eng. **98–99** (2012)